Published in final edited form as:
Langmuir. 2010 December 21; 26(24): 19001–19006. doi:10.1021/la104206h.

Three-dimensional Scaffolds for Tissue Engineering: The Importance of Uniformity in Pore Size and Structure

Sung-Wook Choi[†], **Yu Zhang**, and **Younan Xia**[*]
Department of Biomedical Engineering, Washington University, St. Louis, Missouri 63130, USA

Abstract

To validate the importance of uniformity in pore size and structure of a scaffold for tissue engineering, we fabricated two types of scaffolds with uniform (inverse opal scaffolds) and non-uniform pore sizes and structures, and then evaluated their properties in terms of diffusion of macromolecules, spatial distribution of fibroblasts, and differentiation of preosteoblasts. Our results confirmed the superior performance of the inverse opal scaffolds due to the uniform pore size, homogeneous environment, and high interconnectivity: a higher diffusion rate, a uniform distribution of cells, and a higher degree of differentiation. In addition, we found that both the differentiation of cells and secretion of extracellular matrix were dependent on the properties of the individual pore to which the cells were attached to, rather than the bulk properties of a scaffold. Our results clearly indicate that inverse opal scaffolds could provide a better microenvironment for cells in comparison to a scaffold with non-uniform size and structure.

Keywords

Inverse opal scaffold; pore uniformity; tissue engineering

Introduction

Tissue engineering has emerged as a promising approach to the generation of new tissues for replacing damaged or diseased tissues and/or organs. One of the key components for tissue engineering is the scaffold, which not only provides the necessary support for cells to maintain viability, proliferate, and differentiate into specific cells, but also determines the ultimate shape of the resultant tissue or organ. The attachment, proliferation, and differentiation of cells are strongly affected by the microenvironment associated with a scaffold, including the size, geometry, density of the pores, the windows connecting the pores, and the surface properties.1 Among many issues in tissue engineering, a sufficient supply of oxygen and nutrients throughout a scaffold is considered as a prerequisite to achieve high viability for the cells.2 So far, many research groups have striven to optimize the scaffolds, in an effort to provide the most favorable microenvironment for the cells.3 However, most of the reported scaffolds are characterized by a random pore size and structure with limited interconnectivity, making them less favorable for achieving uniform proliferation and differentiation for the cells. Non-uniform pore structures may produce regions with insufficient concentration of nutrients, which can inhibit proper cellular activities and eventually prevent the formation of homogenous tissues. In addition, conventional techniques for preparing scaffolds remained largely empirical rather than systematic, with limited reproducibility. Furthermore, the pores in conventional scaffolds

[*]Corresponding author. xia@biomed.wustl.edu.
[†]Current address: Division of Biotechnology, The Catholic University of Korea, Gyeonggi-do, Republic of Korea

often have a wide range (e.g., 120–170 μm) of size distribution, making it difficult to accurately define the optimum pore size for cell culture and vascularization. To address these issues, several groups recently developed inverse opal scaffolds with uniform pore sizes and well-interconnected pores and have started to apply them to tissue engineering.4 However, there has been no report on a systematic comparison between scaffolds with uniform and non-uniform pore size and structure in terms of cell viability, proliferation, and differentiation.

Here we demonstrate that a uniform pore size and structure is indeed instrumental in facilitating diffusion of macromolecules, leading to even distribution of cells and homogeneous differentiation of cells. We fabricated two kinds of poly(D, L-lactide-*co*-glycolide) (PLGA) scaffolds with uniform and non-uniform pores, respectively, while the average pore sizes of both scaffolds were adjusted to a scale of 200 μm.5 We then compared their capabilities in terms of diffusion of macromolecules, spatial distribution of fibroblasts, and differentiation of preosteoblasts. Our results clearly established the superior performance of inverse opal scaffolds with a uniform pore size and structure as compared to their counterparts with a non-uniform pore size and structure.

Experimental section

Materials

Gelatin (Type A, from porcine skin, Sigma), sorbitan monooleate (Span® 80, Sigma), and toluene (99.8%, Sigma-Aldrich) were used to produce the uniform microspheres using a simple fluidic device. Poly(D, L-lactide-*co*-glycolide) (PLGA, lactide 75: glycolide 25, M_w ≈ 66,000–107,000, Sigma) and 1,4-dioxane (99.8%, Sigma-Aldrich, the solvent for PLGA) were used as the materials for fabricating the scaffolds. Fluorescein isothiocyanate-dextran (FITC-dextran, M_w ≈ 20,000, Sigma), a hydrophilic dye, was used to evaluate the diffusion rate. All of the chemicals for the preparation of 10 times concentrated simulated body fluid (10XSBF) were purchased from Sigma-Aldrich. The water used in all experiments was obtained by filtering through a set of Millipore cartridges (Epure, Dubuque, IA).

Preparation of scaffolds

Uniform gelatin microspheres and PLGA inverse opal scaffolds were fabricated by modifying our previously reported method.4d›5 Detailed conditions for fabricating uniform gelatin microspheres with average sizes of 224 and 336 μm are presented in Table 1. Non-uniform scaffolds were fabricated using an array of non-uniform gelatin microspheres as a template. The non-uniform gelatin microspheres were produced by gradually changing the flow rate of the continuous phase (toluene) from 0.1 to 3.0 mL/min during the production of gelatin emulsions in the fluidic device while other parameters were kept the same as those for the fabrication of uniform microspheres of 224 μm in diameter. The non-uniform gelatin microspheres in methanol were placed in an oven heated at 65 °C for 2 h to make the template robust enough for handling. All other conditions and procedures were kept the same as those used for the inverse opal scaffolds. Apatite (Ap)-coated PLGA scaffolds were prepared by soaking the PLGA scaffolds in 10XSBF for 2 h with gentle stirring on an orbital shaker.6 The resultant Ap-coated PLGA scaffolds were rinsed with water three times before use.

Measurement of diffusion rates through the scaffolds

A flow cell containing a scaffold was prepared using two 50-mL centrifuge tubes, a PVC tube, and a connector. After slowly pouring 80 mL of water into the centrifuge tube on the right side and the levels of water in both centrifuge tubes were the same, water was introduced into the centrifuge tube on the same side using a syringe pump (KD100, KD

Scientific) at 1.0 mL/min to induce a pressure difference between the two centrifuge tubes. When the flow rate in the sampling tap was stabilized, 0.5 mL of FITC-dextran solution (0.5 wt%) was dropped into the right centrifuge tube and the eluent in the sampling tap was collected every minute and analyzed using a UV-Vis spectrophotometer (Cary 50, Varian)

Cell culture with the inverse opal scaffolds

Mouse fibroblasts (NIH/3T3; ATCC CRL-1658) were used for cell distribution experiments. The cells were maintained in a Dulbecco's Modified Eagle's Medium (DMEM, ATCC), supplemented with 10% fetal bovine serum (FBS, Invitrogen) and 1% antibiotics (containing penicillin and streptomycin, Invitrogen). Prior to cell seeding, the scaffolds were wetted and sterilized by immersion in 70% ethanol for 2 h, washed with PBS (Invitrogen) three times and stored in the culture medium. Approximately 1.6 × 105 cells were used for seeding into each scaffold using a spinner flask (125 mL capacity, Proculture^{TM}, Corning) at 65 rpm for 2 h at 37 °C and 5% CO_2. The cell-seeded scaffolds were then transferred to 24-well plates (one scaffold per well). The cultures were maintained in an incubator at 37 °C in a humidified atmosphere containing 5% CO_2 and the media were changed every other day. At 7 days of culture, culture media were withdrawn, scaffolds were washed with PBS, and the cells were fixed with 3.7% formaldehyde for 20 min. Cell nuclei were then stained with DAPI. Then the cell/scaffold constructs were immersed in 50% sucrose for 1 day. Afterwards, the samples were embedded in O.C.T. compound (Tissue-Tek, Ted Pella) and horizontally sectioned using a microtome (Cryostat, model Microm HN505E) until the middle plane (around 500 μm in depth from the surface into the scaffold) of a construct was exposed. The sectioned constructs were observed using a fluorescence microscope (Axioskop 2, Carl Zeiss).

Mouse calvaria-derived, preosteoblastic cells (MC3T3-E1; ATCC CRL-2593) were used for the experiments of differentiation. The cells were maintained in an α-minimum essential medium (α-MEM, without L-ascorbic acid, Invitrogen), supplemented with 10% FBS and 1% antibiotics (containing penicillin and streptomycin, Invitrogen). The procedures for scaffold sterilization and cell seeding were the same as for the fibroblasts. The cell-seeded scaffolds were then transferred to 24-well plates (one scaffold per well) and cultured in an osteogenic medium supplemented with 300 μM L-ascorbic acid (Sigma-Aldrich) and 10 mM β-glycerol phosphate (Sigma-Aldrich). The cultures were maintained in the incubator at 37 °C in a humidified atmosphere containing 5% CO_2 and the media were changed every other day.

Alkaline phosphatase (ALP) assays were performed at 7, 14, and 28 days after cell seeding using p-nitrophenyl phosphate (pNPP). Briefly, at a specific time point, scaffolds (n = 3 per group per time point) were washed with PBS twice and the cells were lysed in 1 mL of PBS containing 0.1 M glycine, 1 mM $MgCl_2$ and 0.05% Triton X-100 (Sigma). Cell lyses were stored at −20 °C until use. pNPP solution (1 mg/mL) in 0.2 M Tris buffer was made from SIGMAFAST^{TM} pNPP tablets (Sigma) according to the manufacturer's instructions. Reactions were carried out in a 96-well plate by adding 200 μL of pNPP solution and 50 μL of cell lyses to each well, and the plate were kept at 37 °C for 2 h. Absorbance was measured at 405 nm of wavelength using a spectrophotometer immediately after reactions.

Optical microscope (Axioskop 2, Carl Zeiss) and scanning electron microscope (SEM, Nova NanoSEM 2300, FEI) were used to characterize the cell/scaffold constructs (n = 3 per group per time point). For SEM, the cells were fixed with 3.7% formaldehyde for 20 min and dehydrated in a graded ethanol series, followed by sputter-coating with gold for 1 min.

Statistics

Experimental results were expressed as means ± standard deviation (s.d.) of the means of the samples. Statistical comparisons were evaluated by ANOVA, and statistical significance was accepted at $p<0.05$.

Results and Discussion

The procedure for fabricating inverse opal scaffolds include four major steps:4d *i*) production of uniform gelatin microspheres with a fluidic device, *ii*) crystallization of the gelatin microspheres into a cubic-close packed (ccp) lattice, followed by heat treatment to interconnect the microspheres with surrounding ones and improve the mechanical strength of the lattice, *iii*) infiltration of PLGA solution into the void space in the gelatin lattice, and *iv*) freeze-drying followed by selective removal of the gelatin microspheres with warm water. The inverse opal scaffolds have a uniform pore size and structure determined by the uniformity in size for the gelatin microspheres and the crystalline lattice. To fabricate non-uniform scaffolds, we produced gelatin microspheres with sizes in the range of 73 to 388 μm by gradually changing the flow rate of the continuous phase during the formation of gelatin emulsion in the fluidic device while all other parameters were kept the same as those for the uniform gelatin microspheres. For the uniform gelatin microspheres, heat treatment at 65 °C for 1 h was enough to obtain a robust lattice by inducing fusion between microspheres at their junctions. In contrast, for the lattice composed of non-uniform gelatin microspheres, it easily fell apart into small pieces even though it underwent the same procedure for heat treatment. In this case, a longer time (at least 2 h) of heat treatment was necessary to make the lattice robust enough for handling. This observation suggested that the areas and number of contact junctions between the non-uniform gelatin microspheres were rather small, corresponding to a limited size and number of windows connecting the pores in a non-uniform scaffold.

Figure 1, a and b, show SEM images of PLGA scaffolds derived from the uniform and non-uniform gelatin microspheres, respectively. The scaffold prepared using the non-uniform gelatin microspheres exhibited a non-uniform and randomly arranged pore structure with an average pore size of 202 ± 94 μm, together with a relatively small size and number of interconnecting windows (Fig. 1, c and d). By contrast, the inverse opal scaffold showed a uniform pore size of 205 μm with a long-range ordered and well-controlled interconnectivity. The average diameter of the windows (36 ± 22 μm) in the non-uniform scaffold was much smaller than that (66 ± 7 μm) in the inverse opal scaffold because the window size is mainly determined by the smaller one of two adjacent microspheres. Both the pores and the windows serve as pathways for cell migration and nutrient/waste transportation. Therefore, an ideal scaffold should possess a high degree of interconnectivity and a suitable pore size that both enhance the transportation of nutrients/metabolic wastes and prevent pore occlusion during tissue formation. In some cases, the interconnectivity has been shown to have a greater impact than pore size on cell behavior.7

To evaluate the diffusion rate of macromolecules through the scaffold, we designed a simple flow cell using two 50-mL centrifuge tubes and a connector (Fig. 2a). Fluorescein isothiocyanate (FITC)-dextran ($M_w \approx 20k$) was employed as a model macromolecule in place of a protein nutrient. The concentration of FITC-dextran passing through the scaffold was determined by collecting the eluent in a sampling tap and measuring its absorbance by UV-vis spectroscopy. Control experiments were also conducted in the absence of any scaffold in the flow cell. The diffusion rate was calculated from the slope by regressing the linear portion of each curve. As shown in Figure 2b, the diffusion rate of FITC-dextran through the inverse opal scaffolds (slope=0.035) was slightly lower than that for the control sample (slope=0.037). By contrast, the diffusion rate through the non-uniform scaffolds

(slope=0.022) was much lower than that for the inverse opal scaffolds, together with a lag time of ~2 min, which can be attributed to the dominance of small pores and windows in the scaffolds.8 The high diffusion rate of FITC-dextran confirmed a uniform pore size and well-interconnected pore structure inside the inverse opal scaffolds, suggesting an efficient pathway for the transportation of nutrients and metabolic wastes throughout the scaffolds.8 Note that the broad error ranges for the non-uniform scaffolds also suggest a large difference in pore size and structure among the samples and thus low reproducibility for scaffold fabrication.

As many researchers have pointed out,9 a large population of cells concentrated at the perimeter of a scaffold is a major obstacle for generating a uniform tissue with high viability. The cells at the perimeter could exhaust oxygen and nutrients, and thus limit their transportation into the interior of a scaffold, eventually resulting in cell necrosis inside the scaffold. Therefore, an even distribution of cells throughout a scaffold can prevent cell necrosis inside the scaffold and facilitate uniform distribution of soluble signaling molecules for cell-cell communications.10 This issue can be addressed by improving the design of microstructure for a scaffold. To examine the distribution of cells in a scaffold, we seeded fibroblasts into each type of scaffolds. At 7 days of culture, we used 4'-6-diamidino-2-phenylindole (DAPI) to stain the nuclei of the cells in the scaffolds and then sectioned the cell/scaffold constructs using microtome until the middle plane (around 500 μm in depth from the surface into the scaffold) of the construct was exposed. Figure 3, a and b, show fluorescence micrographs taken from cross-sections at the middle plane of the constructs after 7 days of culture, where blue dots indicate cells in the scaffold. It is clear that the cells were uniformly distributed throughout the inverse opal scaffold, whereas the cells in the non-uniform scaffold showed a poor uniformity. A quantitative analysis of cell numbers from the fluorescence micrographs confirmed a more uniform distribution of cells in the inverse opal scaffold than in the non-uniform scaffold (Fig. 3, c and d). The uniform distribution of cells can be attributed to the uniform pores and large windows for the inverse opal scaffold, both of which can facilitate the seeding efficiency, migration of cells, and transportation of nutrients and wastes.

In general, the differentiation of cells is regulated by the morphology, geometry, and surface properties of a scaffold.11 To elucidate the effects of pore size and uniformity on the differentiation of preosteoblasts, we prepared three kinds of apatite (Ap)-coated PLGA scaffolds: non-uniform scaffolds with an average pore size of slightly over 200 μm and inverse opal scaffolds with pore sizes of 211 and 313 μm, respectively. We seeded preosteoblasts into each type of scaffolds, cultured in an osteogenic medium, and evaluated the amounts of secreted extracellular matrix (ECM) and ALP activity during culture. An Ap-decorated surface12 and a pore size of around 200 μm13 are known as optimal conditions for osteogenic induction. In a previous study,14 we have demonstrated that, for inverse opal scaffolds with uniform pore size and structure, PLGA/hydroxyapatite composite scaffolds coated with apatite were more osteo-inductive than both the PLGA/hydroxyapatite composite scaffolds and pristine PLGA scaffolds.

Figure 4a shows an optical micrograph of a pristine Ap-coated inverse opal scaffold with a pore size of 211 μm. At 28 days of culture, a large amount of mineral was found in this inverse opal scaffold (Fig. 4b), whereas very little mineral was observed in the inverse opal scaffold with a pore size of 313 μm (Fig. 4c) and in the non-uniform scaffold (Fig. 4d). Since mineral was observed in the entire inversed opal scaffold with a pore size of 211 μm, it can be concluded that there was uniform differentiation for the preosteoblasts and subsequent secretion of mineral from the cells.

Figure 5 shows SEM images of the preosteoblast/scaffold constructs at 28 days of culture. A large amount of complex of inorganic and organic ECM was found inside all the pores of the inverse opal scaffold with a pore size of 211 μm (Fig. 5a). By contrast, very little mineral without fibrous organic ECM was deposited on the wall of the inverse opal scaffold with a pore size of 313 μm (Fig. 5b). Interestingly, a moderate amount of mixture of inorganic and organic ECM was observed in the large pores (around 200 μm) of the non-uniform scaffold, whereas most of the small pores in the scaffold were occluded by the fibrous organic ECM (Fig. 5c). These observations suggested that the Ap-decorated pores with sizes of around 200 μm could facilitate the secretion of both inorganic and organic ECMs. In contrast, the large pores (around 300 μm) were favorable for the secretion of inorganic ECM and the small pores were favorable for the secretion of organic fibrous ECM. Therefore, we can conclude that the Ap-decorated pores with a uniform size of around 200 μm would provide the most favorable microenvironment for the differentiation of preosteoblasts. More importantly, the secretion pattern of the cells could be largely controlled by tailoring the properties of an individual pore that the cells attached to, rather than the bulk properties of a scaffold (e.g., the average pore size). The significant dependence of secretion pattern on the pore size emphasizes the importance of a precise control over the pore size. Similar to our findings, Kuboki *et al*. have demonstrated the effect of pore size on the pattern of tissue formation by subcutaneously implanting hydroxyapatite scaffolds with different pore sizes (90–120 and 350 μm in diameter) in rats. Their results showed an initial chondrogenesis and subsequent formation of bone tissue in the scaffolds with small pores and direct bone formation with no cartilage intermediate in the scaffolds with large pores.15

We also quantitatively evaluated the differentiation of preosteoblasts in the scaffolds using assays based on ALP activity. ALP is a well-known indicative marker for osteogenic differentiation.16 As shown in Figure 6, there was no significant difference in ALP activities among the samples at 7 days of culture. However, the inverse opal scaffolds with a pore size of 211 μm showed significantly higher ALP activity than the other scaffolds at 14 and 28 days of culture, while there was still no significant difference in ALP activities between the non-uniform scaffolds and the inverse opal scaffolds with a pore size of 313 μm. The ALP test quantitatively confirmed the better performance of the inverse opal scaffolds with a pore size of around 200 μm for the differentiation of preosteoblasts.

Conclusions

We have fabricated scaffolds with uniform and non-uniform, respectively, pore size and structure, and then compared their capabilities in terms of diffusion of macromolecules, spatial distribution of fibroblasts, and differentiation of preosteoblasts. We observed a higher diffusion rate for large molecules, a more uniform distribution of cells, and a higher degree of differentiation in the inverse opal scaffolds, confirming that a uniform pore size and structure can provide more favorable microenvironments for cells than the non-uniform counterparts. In addition, the inverse opal structure has been reported with a relatively higher compressive stiffness.4c,17 We have also found that the secretion pattern of cells could be regulated by varying the pore size of the scaffolds, which provides another reason for the use of inverse opal scaffolds in tissue engineering. Unlike other scaffold systems, we can precisely define and control the pore size and routinely fabricate almost identical scaffolds with high reproducibility. Taken together, we believe that the inverse opal scaffolds should have a bright future in tissue engineering and regenerative medicine.

Acknowledgments

This work was supported in part by an NIH Director's Pioneer Award (5DP1 OD000798) and startup funds from Washington University in St. Louis. Part of the work was done at the Nano Research Facility (NRF), a member of the National Nanotechnology Infrastructure Network (NNIN) that is supported by the NSF under award no. ECS-0335765.

References

1. (a) Hollister SJ. Nat. Mater. 2005; 4:518–524. [PubMed: 16003400] (b) Flemming RG, Murphy CJ, Abrams GA, Goodman SL, Nealey PF. Biomaterials. 1999; 20:573–588. [PubMed: 10213360] (c) Webster TJ, Ergun C, Doremus RH, Siegel RW, Bizios R. Biomaterials. 2000; 21:1803–1810. [PubMed: 10905463] (4) Tampieri A, Celotti G, Sprio S, Delcogliano A, Franzese S. Biomaterials. 2001; 22:1365–1370. [PubMed: 11336309]
2. (a) Li S, De Wijn JR, Li J, Layrolle P, De Groot K. Tissue Eng. 2003; 9:535–548. [PubMed: 12857421] (b) Botchwey E, Dupree MA, Pollack SR, Levine EM, Laurencin CT. J. Biomed. Mater. Res. A. 2003; 67:357–367. [PubMed: 14517896] (c) Grimm MJ, Williams JL. J. Biomech. 1997; 30:743–745. [PubMed: 9239556] (d) Radisic M, Euloth M, Yang L, Langer R, Freed LE, Vunjak-Novakovic G. Biotechnol. Bioeng. 2003; 82:403–414. [PubMed: 12632397]
3. Li Y, Yang S-T. Biotechnol. Bioprocess Eng. 2001; 6:311–325.
4. (a) Zhang Y, Wang S, Eghtedari M, Motamedi M, Kotov NA. Adv. Funct. Mater. 2005; 15:725–731. (b) Kotov NA, Liu Y, Wang S, Cumming C, Eghtedari M, Vargas G, Motamedi M, Nichols J, Cortiella J. Langmuir. 2004; 20:7887–7892. [PubMed: 15350047] (c) Stachowiak AN, Bershteyn A, Tzatzalos E, Irvine DJ. Adv. Mater. 2005; 17:399–403. (d) Choi S-W, Xie J, Xia Y. Adv. Mater. 2009; 21:2997–3001. [PubMed: 19710950] (e) Zhang K, Yan H, Bell DC, Stain A, Francis LF. J. Biomed. Mater. Res. 2003; 66A:860–869. (f) Melde BJ, Stein A. Chem. Mater. 2002; 14:3326–3331. (g) Zhang K, Washburn NR, Simon CG. Biomaterials. 2005; 26:4532–4539. [PubMed: 15722122]
5. Choi S-W, Cheong IW, Kim JH, Xia Y. Small. 2009; 5:454–459. [PubMed: 19189332]
6. Li X, Xie J, Yuan X, Xia Y. Langmuir. 2008; 24:14145–14150. [PubMed: 19053657]
7. Chang BS, Lee C-K, Hong K-S, Youn H-J, Ryu H-S, Chung S-S, Park K-W. Biomaterials. 2000; 21:1291–1298. [PubMed: 10811311]
8. Chor MV, Li W. Meas. Sci. Technol. 2007; 18:208–216.
9. (a) Godbey WT, Hindy SB, Sherman ME, Atala A. Biomaterials. 2004; 25:2799–2805. [PubMed: 14962558] (b) Nieponice A, Soletti L, Guan J, Deasy BM, Huard J, Wagner WR, Vorp DA. Biomaterials. 2008; 29:825–833. [PubMed: 18035412] (c) Mauney JR, Blumberg J, Pirun M, Volloch V, Vunjak-Novakovic G, Kaplan DL. Tissue Eng. 2004; 10:81–92. [PubMed: 15009933]
10. Lee J, Shanbhag S, Kotov NA. J. Mater. Chem. 2006; 16:3558–3564.
11. (a) Meinel L, Fajardo R, Hofmann S, Langer R, Chen J, Snyder B, Vunjak-Novakovic G, Kaplan D. Bone. 2005; 37:688–698. [PubMed: 16140599] (b) Zeltinger J, Sherwood JK, Graham DA, Mueller R, Griffith LG. Tissue Eng. 2001; 7:557–572. [PubMed: 11694190] (c) Liu H, Roy K. Tissue Eng. 2005; 11:319–330. [PubMed: 15738685] (d) Poznansky MC, Evans RH, Foxall RB, Olszak IT, Piascik AH, Hartman KE, Brander C, Meyer TH, Pykett MJ, Chabner KT, Kalams SA, Rosenzweig M, Scadden DT. Nat. Biotechnol. 2000; 18:729–734. [PubMed: 10888839]
12. (a) Yuan H, Kurashina K, de Bruijn JD, Li Y, de Groot K, Zhang XA. Biomaterials. 1999; 20:1799–1806. [PubMed: 10509190] (b) Wang YW, Wu Q, Chen JC, Chen GQ. Biomaterials. 2005; 26:899–904. [PubMed: 15353201]
13. (a) Gogolewski S, Gorna K. J. Biomed. Mater. Res. A. 2007; 80:94–101. [PubMed: 16960827] (b) Srouji S, Kizhner T, Livne E. Regen. Med. 2006; 1:519–528. [PubMed: 17465846]
14. Choi S-W, Zhang Y, Thomopolous S, Xia Y. Langmuir. 2010; 26:12126–12131. [PubMed: 20450216]
15. Kuboki Y, Jin Q, Takita H. J. Bone Joint Surg. 2001; 83A:105–115.
16. Lian JB, Stein GS. Crit. Rev. Oral Biol. Med. 1992; 3:269–305. [PubMed: 1571474]
17. Soentjens SHM, Nettles DL, Carnahan MA, Setton LA, Grinstaff MW. Biomacromolecules. 2006; 7:310–316. [PubMed: 16398530]

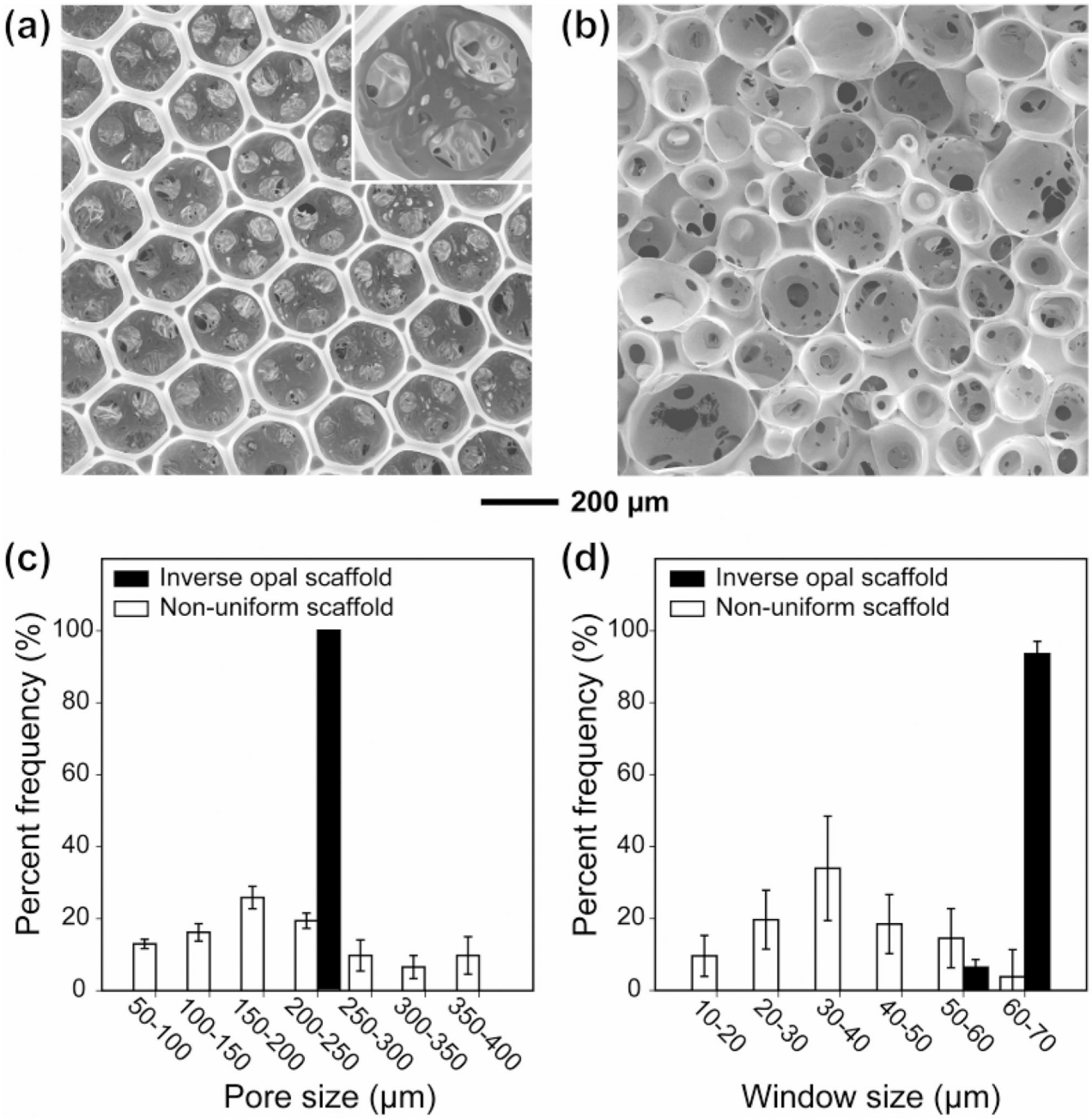

Figure 1.

SEM images of (a) an inverse opal scaffold and (b) a non-uniform scaffold, and size distribution of (c) pores and (d) windows (or the holes connecting adjacent pores) in each scaffold. The black and blank bars correspond to the inverse opal and non-uniform scaffolds, respectively.

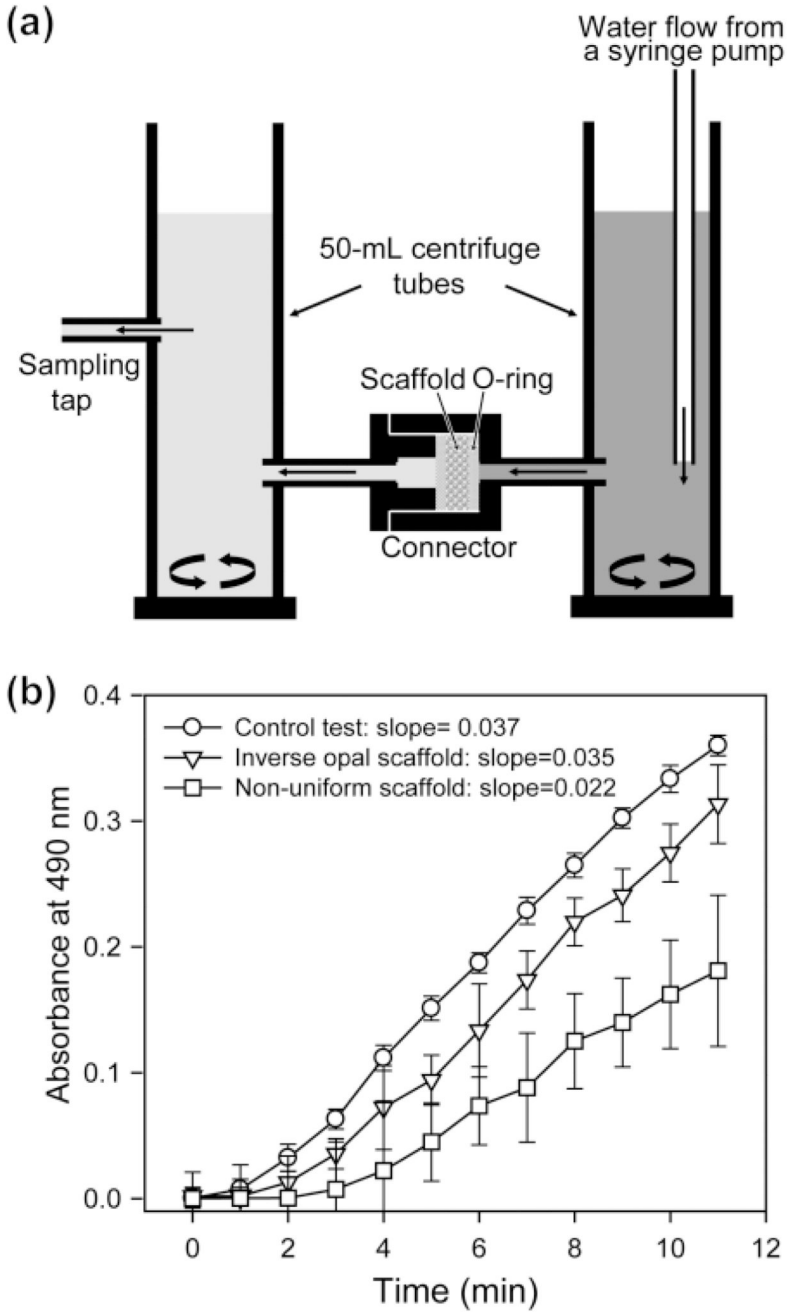

Figure 2.

(a) Illustration of the cell for testing the diffusion of macromolecules passing through a scaffold. (b) Results of diffusion tests (n=3) for FITC-dextran (M_w = 20k) through the scaffolds placed in the specially designed flow cell. The diffusion rate was calculated from the slope by regressing the linear portion of each curve. For the control experiment, no scaffold was placed in the flow cell.

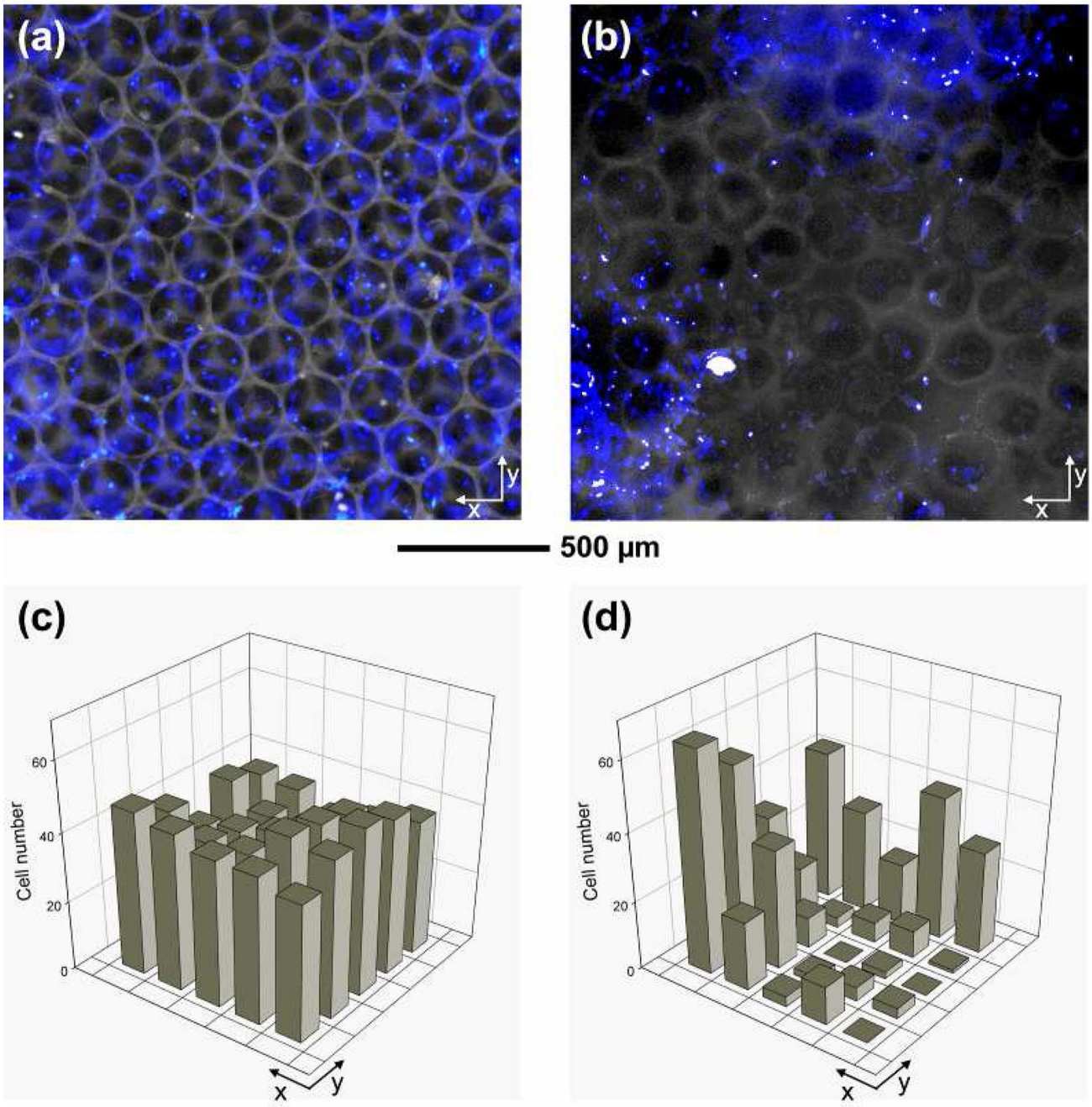

Figure 3.

(a, b) Fluorescence micrographs and (c, d) quantitative analyses of cell numbers after 7 days of culture from the middle plane of (a, c) an inverse opal scaffold with a pore size of 211 μm and (b, d) a non-uniform scaffold. The fibroblast/scaffold constructs were stained with DAPI and then horizontally sectioned using microtome to reach the middle plane approximately 500 μm in depth from the surface of the scaffold. For the plots in (c) and (d), the grid size was $0.3 \times 0.3\ mm^2$.

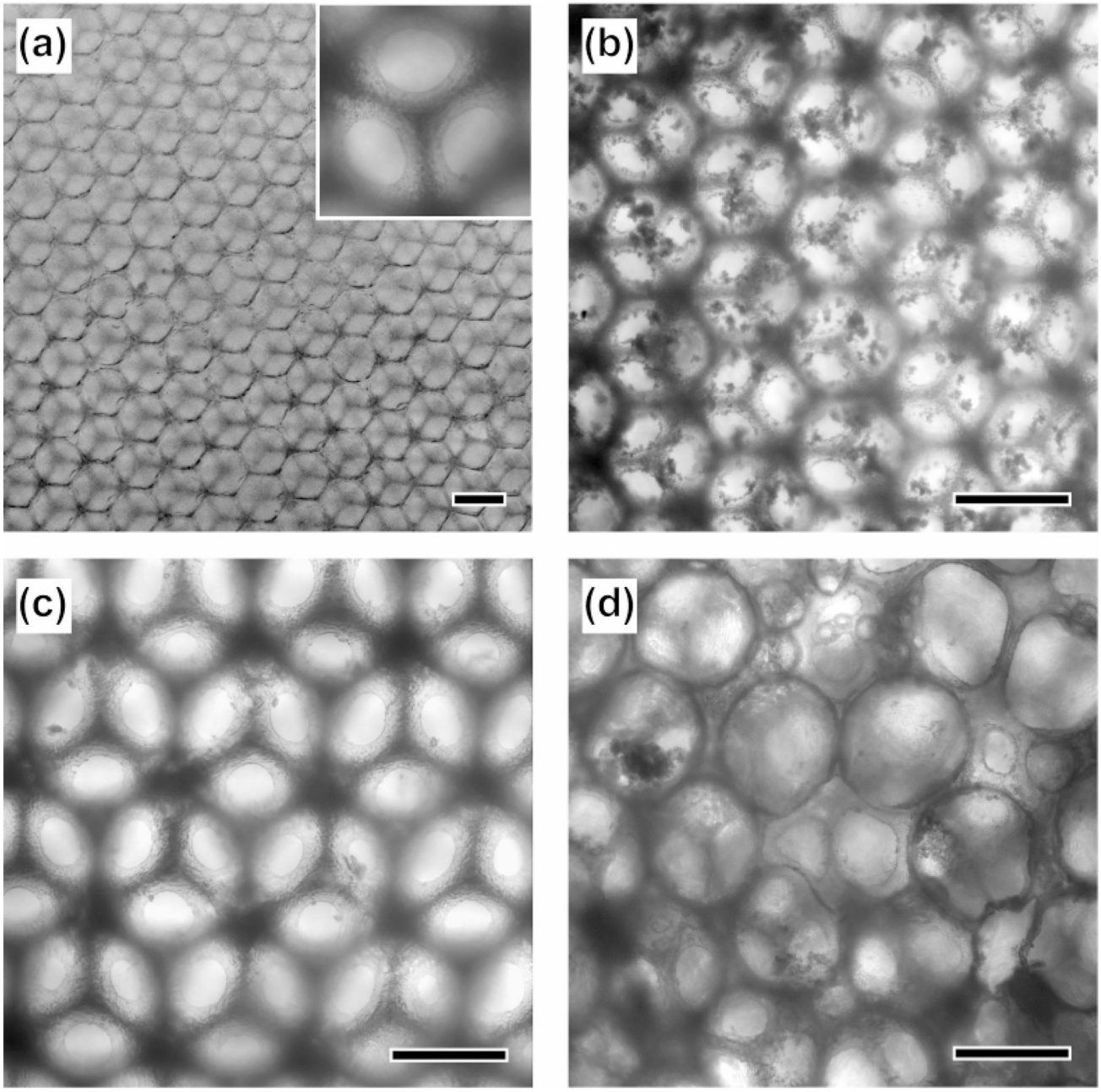

Figure 4.
Optical micrographs of (a) a pristine Ap-coated PLGA scaffold with a pore size of 211 μm, (b-d) preosteoblast/scaffold constructs at 28 days of culture: inverse opal scaffolds with pore sizes of (b) 211 and (c) 313 μm, respectively, and (d) a non-uniform scaffold. Scale bars are 200 μm and the inset in panel (a) is a magnified image of the same sample showing windows connecting the pores.

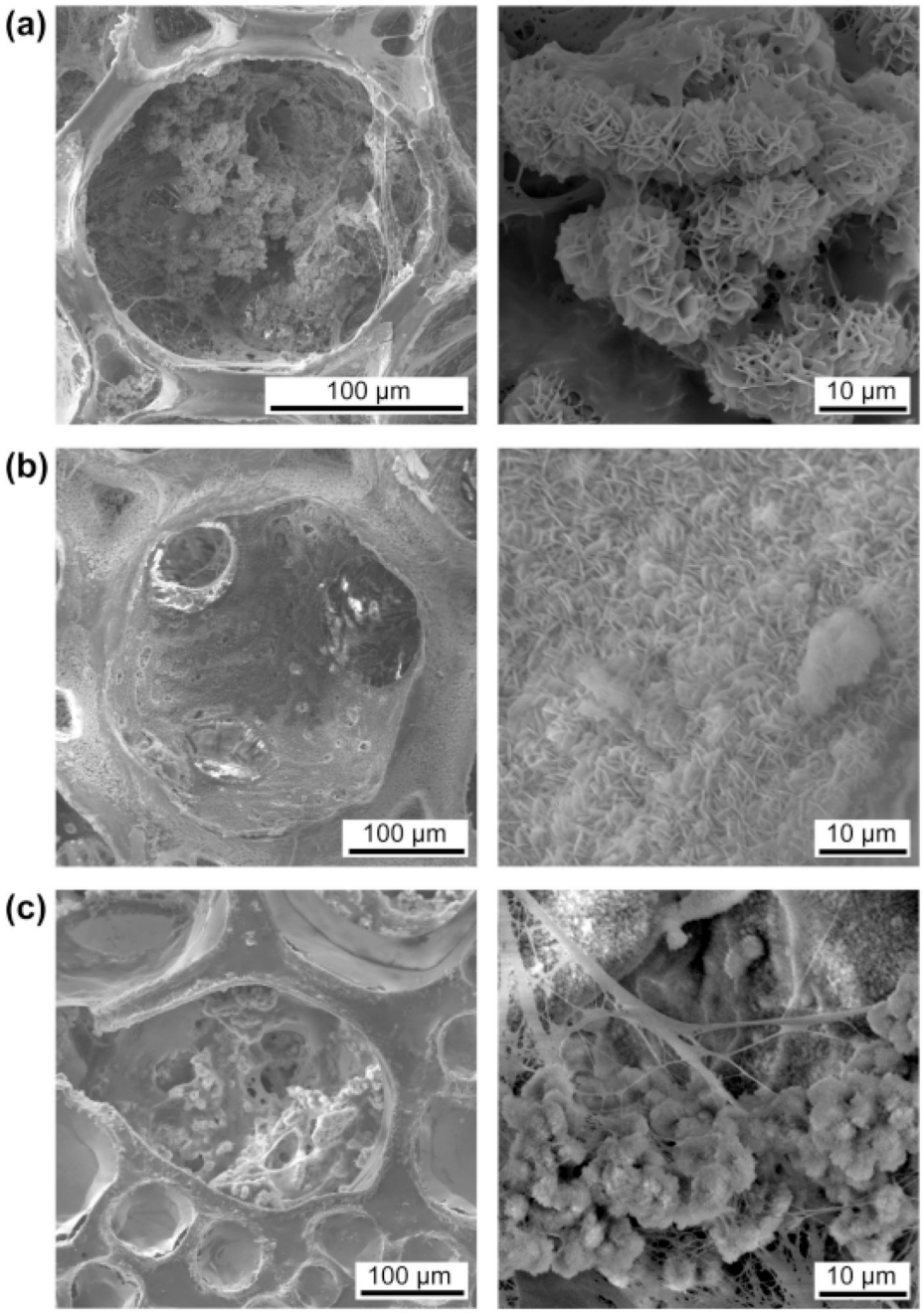

Figure 5.
SEM images of the preosteoblast/scaffold constructs at 28 days of culture: inverse opal scaffolds with pore sizes of (a) 211 and (b) 313 μm, respectively, and (c) a non-uniform scaffold. Magnified views are shown in the right column.

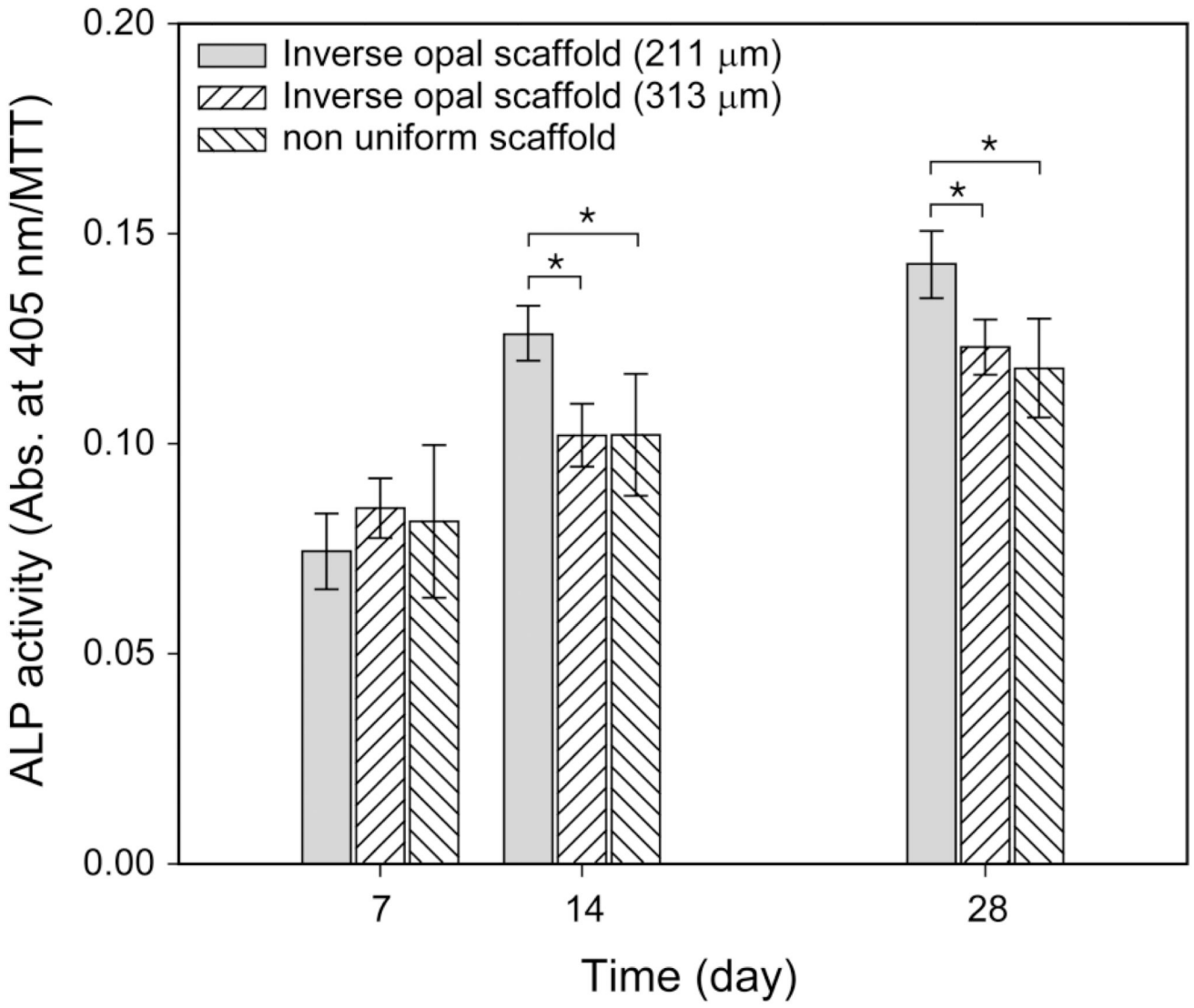

Figure 6.
ALP activities of the preosteoblasts cultured in three different types of Ap-coated PLGA scaffolds at 7, 14, and 28 days of culture. The data are presented as mean ± s.d. (n = 3). * indicates significant difference between the two groups ($p < 0.05$).

Table 1

Experimental parameters for fabrication of gelatin microspheres with a fluidic device.

Microsphere diameter (μm)	Needle (Gauge)	Inner diameter of glass capillary (μm)	Gelatin solution (wt%)	Flow rate (mL/min)	
				Discontinuous phase	Continuous phase
224	26	500	10	0.05	0.2
335	26	800	10	0.05	0.3